

## Excitation and fission decay of $^{238}\text{U}$ using the $(^{17}\text{O}, ^{17}\text{O}')$ reaction

R. L. Auble, J. R. Beene, F. E. Bertrand, J. L. Blankenship, D. J. Horen,  
J. Lisantti,\* and R. L. Varner

*Oak Ridge National Laboratory, Oak Ridge, Tennessee 37831*

A. D'Onofrio

*Oak Ridge National Laboratory, Oak Ridge, Tennessee 37831*

*and Istituto Nazionale de Fisica Nucleare, Napoli, Italy*

(Received 8 November 1989)

The inelastic scattering of 375 MeV  $^{17}\text{O}$  projectiles was used to study the giant resonance region in  $^{238}\text{U}$ . The energy, width, and strength of the giant quadrupole resonance (GQR) were extracted from singles spectra and fission probabilities were deduced from singles and coincidence data. Angular correlations between fission fragments and inelastically scattered particles were measured to search for evidence of  $K$  conservation in the fission decay of the GQR.

### I. INTRODUCTION

Giant resonances in  $^{238}\text{U}$  and, in particular, their fission decay properties have been the subject of a number of recent investigations,<sup>1-8</sup> often with conflicting results. Recent  $(e, e'f)$  measurements<sup>8</sup> have apparently laid to rest the controversy over the fission probability of the isoscalar giant quadrupole resonance (GQR). However, there remain uncertainties in the centroid, width, and strength of the GQR, and the possibility of  $K$  conservation<sup>3,6</sup> in the fission decay of the GQR has not been resolved. The present studies were undertaken to address these points.

### II. EXPERIMENTAL PROCEDURES

The measurements were made using 375 MeV  $^{17}\text{O}$  ions from the coupled accelerators at the Holifield Heavy Ion Research Facility. Scattered particles were detected at the focal plane of the Broad Range Magnetic Spectrograph. An absorber was placed over part of the focal plane detector to keep elastically scattered particles, and most of the particles from transfer reactions, from entering the detector. The energy resolution was approximately 300 keV full width at half maximum (FWHM). The spectrograph was set to accept approximately  $4^\circ$  in the scattering plane and particle trajectories determined by the focal plane detector allowed measurement of the scattering angle to better than  $\pm 0.1^\circ$ . Calibration of the solid angle was obtained by comparing measured elastic scattering cross sections with optical model calculations.

For the coincidence studies, fission fragments were detected by four  $8.2 \times 9.4 \text{ cm}^2$  position-sensitive avalanche detectors which formed a box with sides parallel to, and 6.2 cm from, the beam line. Opposing detectors were offset parallel to the beam line in order to obtain partial coverage of all fission angles (measured relative to the recoil axis). The detectors were arranged to detect both fission fragments for reactions having opening angles near  $180^\circ$  but, due to nonuniform detection

efficiency, for many events only one fragment was detected.

The targets were self-supporting metallic foils of depleted uranium with thicknesses of approximately  $0.50 \text{ mg/cm}^2$ . During the coincidence measurements, the targets were oriented at an angle of  $45^\circ$  to the beam line to minimize shadowing of the fission detectors by the target frame.

### III. SINGLES MEASUREMENTS

Inelastic spectra were taken at spectrograph angle settings of  $10^\circ$  and  $13^\circ$  and a typical spectrum is shown in Fig. 1. The region below about 2 MeV of excitation was eliminated by the absorber in front of the focal plane detectors. A broad peak is observed at about 10 MeV of excitation which, based on comparison with results reported for  $^{208}\text{Pb}$  using  $^{16}\text{O}$  and  $^{17}\text{O}$  projectiles,<sup>9,10</sup> is attributed primarily to the GQR. The peak/background ratio is, however, considerably smaller than for  $^{208}\text{Pb}$ . This can be attributed in part to the higher density of low-lying states in  $^{238}\text{U}$  which results in the strong continuum observed at lower excitation energies. In addition, the GQR is predicted to have a larger width in deformed nuclei due to fragmentation of the resonance into its separate  $K$  components.<sup>11,12</sup>

To obtain the angular distribution for the GQR, the data were divided into  $0.25^\circ$  (lab) angle bins and a least-squares fit was made to each spectrum. The background was constructed from a linear component to fit the region above about 15 MeV plus a skewed-Gaussian to reproduce the low excitation region. The GQR can be fit by either an asymmetric Gaussian skewed to the high energy side, or a symmetric Gaussian plus a second peak at about 13 MeV having a cross section  $\sim 20\%$  of that of the GQR. The second alternative was chosen since it appears reasonable to assume that the peak at 13 MeV can be attributed to the giant monopole resonance. The energy is consistent with values reported<sup>7,8</sup> for  $^{238}\text{U}$  (GMR) and the yield is consistent with the relative  $EO/E2$  cross

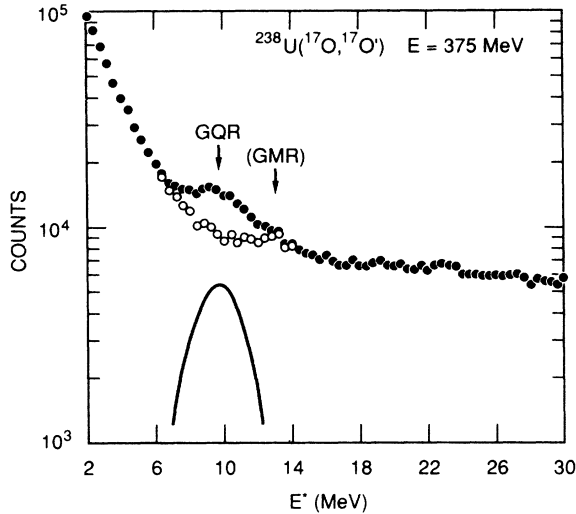


FIG. 1. Singles spectrum from the  $^{238}\text{U}(^{17}\text{O}, ^{17}\text{O}')$  reaction at  $E(^{17}\text{O})=375$  MeV. The solid line is the GQR peak obtained in the least-squares fit and the open circles show the continuum obtained by subtraction of the GQR from the singles spectrum.

sections reported<sup>10</sup> in the  $^{208}\text{Pb}(^{16}\text{O}, ^{16}\text{O}')$  reaction.

Initially, the position and width of the GQR were allowed to vary during the fitting process, resulting in somewhat different values for each angle bin. The average value obtained for the centroid of the GQR was  $9.7 \pm 0.2$  MeV. The widths obtained from these fits displayed larger variations and resulted in an average value of  $3.6 \pm 0.5$  MeV FWHM. The position and width of the GQR were then fixed at the average values to obtain the final peak areas. The resultant cross sections, corrected for spectrograph solid angle and converted to the center-of-mass system, are shown in Fig. 2. The error bars reflect the large uncertainty in the peak width and the decreasing peak/background ratio at  $\theta < 12^\circ$ . An additional uncertainty of  $\pm 10\%$  in the overall normalization is not included. Also shown in Fig. 2 is a coupled-channels prediction for an  $L=2$  transition calculated with the code PTOLEMY.<sup>13</sup> The calculations used a deformed optical potential with  $\beta=0.0845$ , and geometry taken from a study<sup>10</sup> of 400 MeV  $^{16}\text{O}$  scattering from  $^{208}\text{Pb}$ . A deformed nuclear potential with  $\beta_2=0.27$  and  $\beta_4=0.051$  was used for the  $^{238}\text{U}$  nucleus. Only the ground state and GQR were included in these calculations. The predicted shape agrees with the data for  $\theta > 11^\circ$ , but the predicted maximum near  $10^\circ$  is not evident in the data. Comparison of the measured and calculated cross sections over the angular range from  $12^\circ$  to  $16^\circ$  results in a strength of  $(90 \pm 20)\%$  of the  $E2$  energy-weighted sum rule (EWSR) in the 9.7 MeV peak.

The parameters deduced for the GQR are in reasonable agreement with those reported in  $(\alpha, \alpha')$  measurements<sup>4</sup> and recent  $(e, e'f)$  coincidence studies,<sup>8</sup> and with systematics for the GQR.<sup>14</sup> The energy is somewhat lower than the value of  $10.8 \pm 0.3$  MeV reported in  $(\alpha, \alpha')$

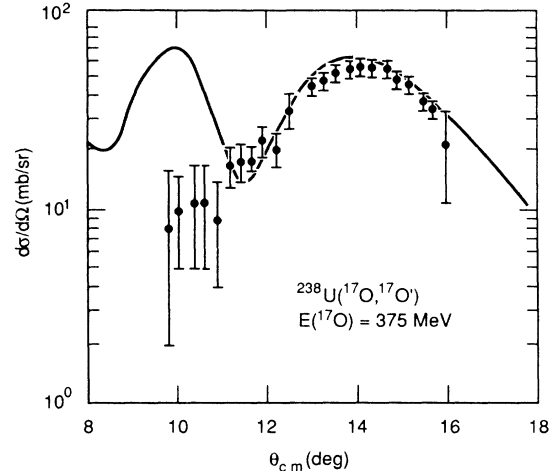


FIG. 2. Comparison of the measured angular distribution for the GQR with a distorted-wave Born approximation prediction assuming 100%  $E2$  EWSR.

but appears to be in good agreement with the  $(e, e'f)$  results. The width agrees, within the experimental uncertainties, with the value of  $3.0 \pm 0.4$  MeV reported in  $(\alpha, \alpha')$  but appears to be significantly broader than the peak observed in  $(e, e'f)$ . The strength obtained in the present study is also larger than that obtained in the  $(\alpha, \alpha')$  measurement which may indicate that other resonances, such as the  $L=4$  resonance reported in  $(\alpha, \alpha')$ , make a significant contribution to the 9.7 MeV peak.

#### IV. COINCIDENCE STUDIES

An inelastic spectrum recorded in coincidence with fission fragments is shown in the upper part of Fig. 3. The complexity of the coincidence spectra, as compared to singles, is due to variation of the fission probability ( $P_f$ ) with excitation energy. The peak near the fission barrier at about 6 MeV and the rise at the threshold for second-chance fission at about 13 MeV are well known features<sup>2-4</sup> of  $^{238}\text{U}$  fission gated spectra. In the intervening region from 7 to 12 MeV there is only a relatively smooth "hump" which cannot be readily decomposed into continuum and resonance components. We can, however, determine the fission probability for the combined continuum plus GQR by dividing the coincidence spectrum, integrated over all fission angles, by the singles spectrum.

The coincidence data were first corrected for the solid angle and detection efficiency of the fission fragment detectors. The solid angle was calculated from the detector geometry and the efficiency corrections were deduced from the ratio of double  $(^{17}\text{O}'f)$  to triplet  $(^{17}\text{O}'ff)$  coincidences. The result is shown in the lower part of Fig. 3. The correction factors varied considerably with fission angle, particularly for  $50^\circ < \theta_f < 70^\circ$  which corresponds to fragments hitting near the edges of the detectors, and introduce an estimated  $\pm 20\%$  uncertainty in the normalization of the coincidence data. The correction factors

were, however, nearly independent of the excitation energy. Thus, with the possible exception of energies near the fission barrier where the angular correlation is sharply peaked around the recoil axis, the dependence of  $P_f$  on excitation energy is believed to be unaffected by these corrections. The results shown in Fig. 3(b) are somewhat smaller than, but otherwise in very good agreement with, values deduced from photofission measurements.<sup>15,16</sup>

The first point to note from Fig. 3(b) is that for energies between about 10 MeV, where the GQR cross section is a maximum in the singles spectrum, and 12 MeV, where the GQR is relatively weak, the fission probability is nearly constant. If  $P_f$  for the continuum is assumed to be constant over this energy range, as found in photofission studies<sup>15</sup> for dipole transitions, then  $P_f$  for the GQR must be nearly identical to that for the continuum, in agreement with the conclusions of Refs. 3 and 8. If  $P_f$  for the GQR and continuum are identical at all excitation energies, then the coincidence spectrum can be decomposed as shown in Fig. 3(a). Here, the GQR and continuum obtained from singles have been multiplied by the fission probabilities shown in Fig. 3(b). Also shown

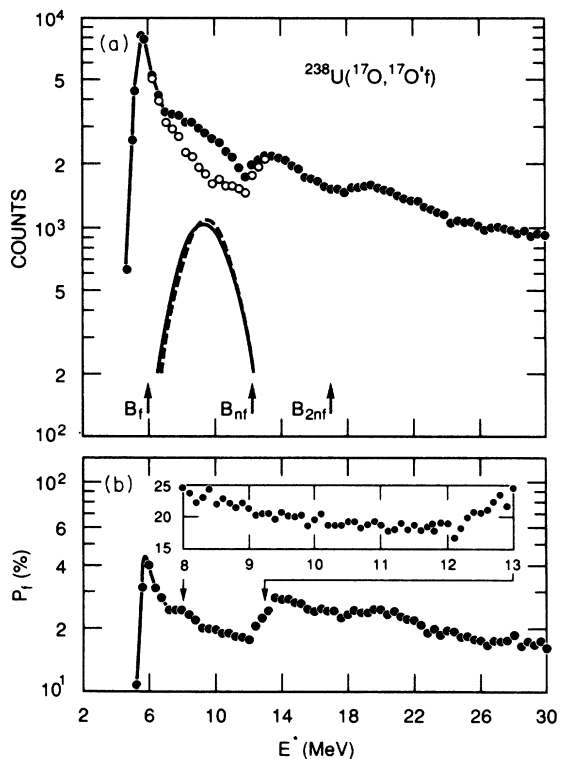


FIG. 3. (a) Spectrum obtained in coincidence with fission fragments integrated over all fission angles (solid points). The open points and the peak shown by the solid line were obtained by multiplying the continuum and GQR peak from singles data by the fission probability shown in (b). The dashed line is the GQR peak shape from singles. (b) Fission probability obtained by dividing the coincidence data by the singles spectrum, with solid angle and efficiency corrections applied as noted in the text. The inset shows the region of the GQR on an expanded energy scale.

for comparison is the GQR peak shape obtained in singles, normalized to the same area as in coincidence. The net effect on the GQR peak is a slight broadening and a shift of the centroid to about 9.5 MeV in the coincidence spectrum. There is no indication of any significant difference in  $P_f$  for the GQR and the continuum at lower excitation energies as one might have expected on the basis of recent statistical model calculations.<sup>17</sup>

The present results are consistent with photofission measurements up to about 14 MeV, but at higher excitation energies  $P_f$  is considerably smaller than the photofission values. A similar effect is also apparent in the results reported<sup>2</sup> for the  $^{238}\text{U}(^6\text{Li}, ^6\text{Li}'f)$  reaction. The most likely explanation for this difference is that in heavy-ion scattering, the energy lost in the reaction is not always due to inelastic excitation of the target nucleus, but includes more complicated reactions which do not lead to fission.

The angular correlation between inelastically scattered particles and fission fragments is a potentially useful means of studying the fission decay process. For excitation energies near the fission barrier, fission fragments are emitted preferentially along the recoil axis<sup>18</sup> due to the dominance of  $K=0$  transition states at the saddle point. With increasing excitation energy, the density of transition states at the saddle point with  $K > 0$  increases, even-

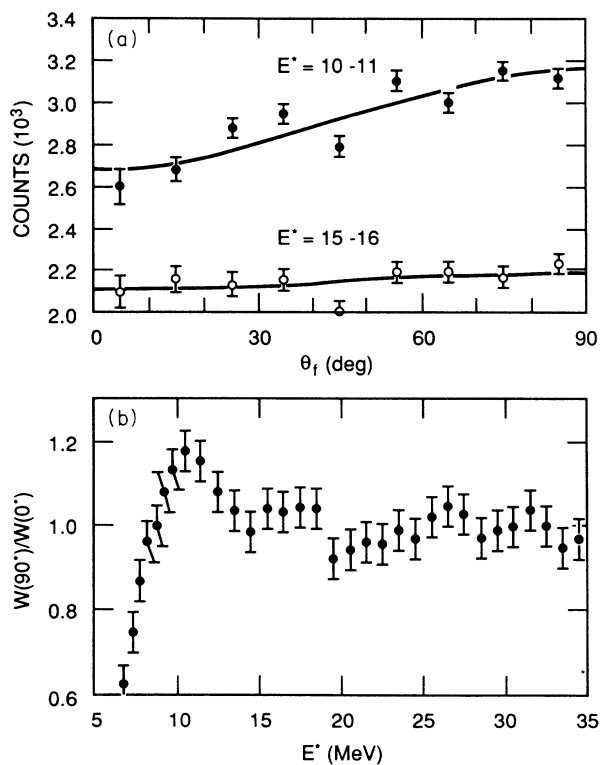


FIG. 4. (a) Angular correlation between inelastically scattered particles and fission fragments for  $E^* = 10-11$  MeV and  $15-16$  MeV. The solid lines are fits to the function  $W(\theta) = A_0 + A_2 \sin^2 \theta$ . (b) Anisotropy,  $W(90)/W(0)$ , as a function of excitation energy. The data were normalized to give isotropy for energies from 25 to 35 MeV.

tually resulting in an isotropic angular correlation.<sup>19</sup>

The absolute cross sections for individual fission fragment angle bins have large uncertainties due to the solid angle and detection efficiency corrections which could mask any small anisotropy that might be present. Therefore, spectra gated by fission fragments emitted in  $10^\circ$  wide angle bins were normalized to give the same number of counts for  $E^*$  between 25 and 35 MeV. The angular correlation for each 0.5 or 1.0 MeV wide excitation energy bin is adequately described by a simple function of the form  $W(\theta) = A_0 + A_2 \sin^2 \theta$ , except for energies near the barrier. The anisotropies,  $W(90)/W(0)$ , obtained from these fits are plotted in Fig. 4. The expected strong anisotropy below about 8 MeV is clearly evident and for energies above about 14 MeV the correlation is isotropic within the experimental uncertainties. However, in the region from 9 to 13 MeV, there appears to be a preference for decay at  $90^\circ$ . The nonuniform efficiency of the fission fragment detectors cast some doubt on this result, but it seems unlikely that the detectors could introduce an anisotropy in such a localized energy region. It is interesting that the asymmetry is largest for energies around 10–12 MeV, i.e., the high energy side of the GQR. This would correspond to the predicted position of the  $K = 2$  component of the GQR, for which the angular correlation would be peaked at  $90^\circ$ . The angular correlations for the 10–11 and 15–16 MeV energy bins are shown at the top of Fig. 4 to indicate the quality of the fits.

A recent  $(e, e'f)$  measurement found that the  $E2$  resonance has a larger symmetric fission component than other resonances.<sup>20</sup> In that study,  $\Gamma_S/\Gamma_A$  has a peak in the region of 10–12 MeV which the authors interpret as an enhanced coupling of the GQR to the fission process. Perhaps the present result is a further indication of unusual fission decay properties of the GQR.

## V. CONCLUSIONS

From the singles measurements, we obtain values of  $9.7 \pm 0.2$  MeV and  $3.6 \pm 0.5$  MeV for the centroid and width of the GQR, respectively, and conclude that the GQR in  $^{238}\text{U}$  exhausts a large fraction ( $90 \pm 20\%$ ) of the  $E2$  energy weighted sum rule. Fission probabilities are consistent with photofission data up to about 14 MeV of excitation and indicate that the fission probability for the GQR is essentially identical to that for the underlying continuum. A small anisotropy is indicated for excitation energies from 10 to 12 MeV which may suggest an anomalous decay mode for the  $K = 2$  component of the GQR.

## ACKNOWLEDGMENTS

Oak Ridge National Laboratory was operated by Martin Marietta Energy Systems, Inc. under Contract No. DE-AC05-84OR21400 with the U.S. Department of Energy.

\*Present address: Indiana University Cyclotron Facility, Milo B. Sampson Lane, Bloomington, IN 47405.

<sup>1</sup>J. D. T. Aruda Neto, S. B. Herdade, B. S. Bhandari, and I. C. Nascimento, Phys. Rev. C **18**, 863 (1978); J. D. T. Arruda-Neto, S. B. Herdade, I. C. Nascimento, and B. L. Berman, Nucl. Phys. **A389**, 378 (1982).

<sup>2</sup>A. C. Shotter, C. K. Gelbke, T. C. Awes, B. B. Back, J. Mahoney, T. J. M. Symons, and D. K. Scott, Phys. Rev. Lett. **43**, 569 (1979).

<sup>3</sup>F. E. Bertrand, J. R. Beene, C. E. Bemis, Jr., E. E. Gross, D. J. Horen, and J. R. Wu, Phys. Lett. **99B**, 213 (1981).

<sup>4</sup>H. P. Morsch, M. Rogge, P. Decowski, H. Machner, C. Sukosd, P. David, J. Debrus, J. Hartfiel, H. Janzen, and J. Schulze, Phys. Lett. **119B**, 315 (1982); H. P. Morsch, M. Rogge, P. Turek, C. Mayer-Boricke, and P. Decowski, Phys. Rev. C **25**, 2939 (1982).

<sup>5</sup>D. H. Dowell, L. S. Cardman, P. Axel, G. Bolme, and S. E. Williamson, Phys. Rev. Lett. **49**, 113 (1982).

<sup>6</sup>K. A. Griffioen, P. J. Countryman, K. T. Knöpfle, K. Van Bibber, M. R. Yearian, J. G. Woodworth, D. Rowley, and J. R. Calarco, Phys. Rev. C **34**, 1375 (1986).

<sup>7</sup>R. De Leo, S. Brandenburg, A. G. Drentje, M. N. Harakeh, H. Janszen, and A. van der Woude, Nucl. Phys. **A441**, 591 (1985).

<sup>8</sup>Th. Weber, R. D. Heil, U. Kneissl, W. Pecho, W. Wilke, H. J. Emrich, Th. Kihm, and K. T. Knöpfle, Phys. Rev. Lett. **59**,

2028 (1987).

<sup>9</sup>F. E. Bertrand, R. O. Sayer, R. L. Auble, M. Beckerman, J. L. Blankenship, B. L. Burks, M. A. G. Fernandes, C. W. Glover, E. E. Gross, D. J. Horen, J. Gomez del Campo, and D. Shapira, Phys. Rev. C **35**, 111 (1987).

<sup>10</sup>T. P. Sjoreen, F. E. Bertrand, R. L. Auble, E. E. Gross, D. J. Horen, D. Shapira, and D. B. Wright, Phys. Rev. C **29**, 1370 (1984).

<sup>11</sup>T. Suzuki and D. J. Rowe, Nucl. Phys. **A289**, 461 (1977).

<sup>12</sup>Y. Abgrall, B. Morand, E. Caurier, and B. Grammaticos, Nucl. Phys. **A346**, 431 (1980).

<sup>13</sup>M. H. Macfarlane and S. C. Pieper, Argonne National Laboratory Report No. ANL-76-11, Rev. 1, 1978.

<sup>14</sup>F. E. Bertrand, Nucl. Phys. **A354**, 129 (1981).

<sup>15</sup>A. Veyssièrè, H. Beil, R. Bergère, P. Carlos, A. Lepretre, and K. Kernbath, Nucl. Phys. **A199**, 45 (1973).

<sup>16</sup>O. Y. Mafra, S. Kuniyoshi, and J. Goldemberg, Nucl. Phys. **A186**, 110 (1972).

<sup>17</sup>H. Dias, J. D. T. Arruda-Neto, B. V. Carlson, and M. S. Hussein, Phys. Rev. C **39**, 564 (1989).

<sup>18</sup>H. C. Britt and F. Plasil, Phys. Rev. **144**, 1046 (1966).

<sup>19</sup>R. Vandenbosch and J. R. Huizenga, *Nuclear Fission* (Academic, New York, 1973).

<sup>20</sup>Th. Weber, R. D. Heil, U. Kneissl, W. Wilke, H. J. Emrich, Th. Kihm, and K. T. Knöpfle, Phys. Rev. Lett. **62**, 129 (1989).